ELSEVIER

Ultramicroscopy 71 (1998) 205–212

ultramicroscopy

Carrier trapping into single GaAs quantum wires studied by variable temperature near-field spectroscopy

A. Richter[a], M. Süptitz[a], Ch. Lienau[a,*], T. Elsaesser[a], M. Ramsteiner[b], R. Nötzel[b], K.H. Ploog[b]

[a] *Max-Born-Institut für Nichtlineare Optik und Kurzzeitspektroskopie, D-12489 Berlin, Germany*
[b] *Paul-Drude-Institut für Festkörperelektronik, D-10117 Berlin, Germany*

Abstract

The trapping of carriers into single GaAs quantum wires is studied by near-field luminescence and luminescence excitation spectroscopy with a spatial resolution of 250 nm. The formation of the investigated GaAs wires relies on a new growth mode in the preferential migration of Ga atoms on patterned (3 1 1)A GaAs surfaces. Near-field photoluminescence excitation spectroscopy allows for a separation of quantum wire and well absorption and gives evidence of slight potential barriers in the vicinity of the quantum wire. At room temperature, carriers locally excited in the quantum well undergo real-space transfer over several micrometers, pass the barriers and are trapped into the quantum wire via phonon emission. At temperatures below 20 K, real-space transfer through the barriers is suppressed and only carriers generated in the vicinity of the quantum wire get trapped into bound states.

PACS: 78.66.Fd; 78.55.Cr; 07.60.Pd

Keywords: Scanning optical microscopy; Quantum wires; Photoluminescence; Spectroscopy; Near-field optics

1. Introduction

In recent years, low-dimensional semiconductor nanostructures such as one-dimensional quantum wires or zero-dimensional quantum dots have received much interest. This interest arose in part from the desire to design laser devices with improved optical characteristics such as higher optical gain, ultra-low threshold current and narrow spectral line widths [1, 2]. Moreover, unique new physical properties such as narrowed densities of states, increased excitonic effects [3–6], strongly enhanced carrier mobilities [7] and modified phonon scattering rates [8] are predicted for low-dimensional systems.

Since the dimensions of such nanostructures are typically between 1 and 100 nm, their characterization, which is mandatory for understanding and optimizing their properties, requires sophisticated experimental techniques providing very high spatial resolution. While non-optical methods such as

* Corresponding author. E-mail: lienau@mbi-berlin.de

0304-3991/98/$19.00
PII S0304-3991(97)00073-9

scanning or transmission electron microscopy, scanning tunneling and atomic force microscopy are readily available, these dimensions are far beyond the resolution limit of classical optical techniques. Thus, so far, the optical properties of low-dimensional semiconductors have mainly been studied with ensembles consisting of up to hundreds of nanostructures. In such experiments, size fluctuations within the ensemble lead to a strong inhomogeneous broadening of the optical spectra and make the observation of the intrinsic low-dimensional behavior difficult. Here, optical techniques with resolution in the 100 nm range, such as near-field scanning optical microscopy (NSOM) have the potential to select *single* nanostructures and thus to provide entirely new information on their physical properties. This potential has been demonstrated in pioneering near-field spectroscopic experiments on quantum wells [9] and wires [10]. Very recently, the absorption properties of single quantum wires have been investigated for the first time using near-field spectroscopy [11].

In contrast to the steady-state optical properties, the carrier dynamics in single quantum wires has not been addressed so far by near-field optical techniques. Here, experiments with high spatial resolution allow for a separation of different microscopic processes like real-space transfer and carrier capture. In this paper, we present the first variable temperature NSOM study of carrier dynamics in single quantum wires. The experiments are performed on a novel type of GaAs quantum wires formed by a new growth mode in the preferential migration of Ga atoms on patterned (3 1 1)A GaAs surfaces [12, 13]. The focus of this paper is on analyzing the microscopic mechanisms of carrier trapping from the embedding GaAs quantum well (QW) into the sidewall quantum wire (QWR) structure. Photoluminescence excitation spectroscopy with a spatial resolution of 250 nm allows for a clear separation of QWR and QW absorption and gives information on the local band-gap profile of the embedding QW. The QWR is shown to be surrounded by shallow energetic barriers that separate QWR and flat area QW. At low temperatures, these barriers play an important role for the carrier-capture process. Trapping of carriers that are locally generated within the flat area QW is prevented by the barriers and trapping only occurs for local excitation near the QWR. At room temperature, thermal activation across the barriers becomes possible, and carrier trapping is preceded by real-space transfer of carriers in continuum QW states occuring over a length of several micrometers.

2. Experimental

The structure of the investigated QWR sample is shown schematically in Fig. 1a. The sample was grown by molecular beam epitaxy on patterned GaAs (3 1 1) substrates along the sidewall of 15–20 nm high mesa stripes oriented along [01 – 1]. The GaAs substrate was patterned by using optical lithography and wet chemical etching. The nanostructure consists of a 50 nm thick GaAs buffer layer, a 50 nm $Al_{0.5}Ga_{0.5}As$ lower-barrier layer and a nominally 6 nm thick GaAs-quantum

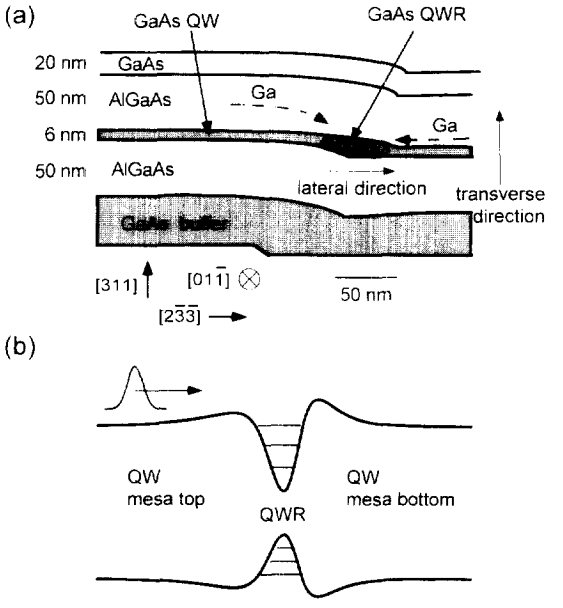

Fig. 1. (a) Schematic of the quantum wire structure. The one-dimensional confinement originates from the thickness variation of the GaAs quantum well along the lateral [2 3 3] direction. (b) Schematic energy diagram: potential energy and subband structure along the lateral direction. Diffusion of carriers excited in the quantum well is depicted schematically.

well (QW) layer. This GaAs layer is covered with a 50 nm $Al_{0.5}Ga_{0.5}As$ upper barrier and a 20 nm GaAs cap layer. During growth, a sidewall QWR is formed in this sample by the preferential migration of Ga atoms within the QW layer towards the sidewall. Cross-sectional TEM images indicate that due to this Ga migration process the thickness of the GaAs QW at the sidewall increases up to 13 nm, resulting in a 1D confinement over a lateral QWR width of about 50 nm. The confinement energies of electrons and holes with respect to the surrounding 6 nm QW are about 60 and 15 meV, respectively, as is indicated in the schematic energy diagram shown in Fig. 1b.

Near-field optical spectra of a single QWR are presented at sample temperatures of 8 and 300 K. The room temperature near-field scanning optical microscope (NSOM) is based on a commercial instrument (Topometrix Aurora), while a new home-built variable temperature microscope which is described in detail elsewhere [14] is used for the low-temperature experiments. Spatially resolved optical excitation of the sample was achieved by transmitting light through a nanometer-sized aperture located at the end of a standard NSOM probe tip. Such tips were made by pulling single-mode optical fibers to a sharp taper in a commercial fiber puller and then coating the taper with a 50 to 100 nm thick aluminum or gold layer. The diameter of the aperture at the very end of the taper was varied between less than 100 and 300 nm. Photoluminescence emitted by the sample was collected with a standard microscope objective in reflection geometry. The photoluminescence was dispersed in a 0.25 m double monochromator with a spectral resolution of 1.2 nm and detected with a (time correlated) single-photon counting system based on a silicon avalanche photodiode detector (Si-APD). In the experiments, the photoluminescence is detected as a function of the tip position relative to the sample. The tip-to-sample distance is controlled by either using a modified version of the optical shear force setup proposed by Refs. [15, 16] or a tuning fork setup [17]. Shear-force images, i.e. images of the z-piezo voltage as a function of tip position, provide direct information about the topography of the sample surface and were recorded simultaneously with the near-field photoluminescence images. The scan range in these experiments was typically $10 \times 10\ \mu m^2$ and 100×100 or 200×200 data points were recorded for each scan. A diode pumped continuous wave Cr^{3+} : LiSAF laser, tunable between 810 and 860 nm, a home-built femtosecond Ti:sapphire laser tunable between 750 and 860 nm and a HeNe laser were used as excitation sources.

3. Optical spectra and local band-gap mapping

Near-field photoluminescence excitation (PLE) spectroscopy is used to resolve the local energetics of the QWR and the embedding QW structure. Fig. 2a shows a room-temperature near-field PLE spectrum as a function of excitation energy E_{ex} and of the lateral separation between the fiber tip and the QWR located at $y = 0$. Here, the sample was locally excited by transmitting light through the NSOM probe and the far-field luminescence was detected at an energy of 1.459 eV, i.e. at the maximum of the QWR emission at room temperature. The tip was scanned along the lateral y-direction perpendicular to the wire structure. For photon energies below 1.52 eV, photoexcitation occurs exclusively in a narrow region along $y = 0$, i.e. at the location of the QWR. The width of this area (FWHM) has a value of about 260 nm and is limited by the specific sample structure. Details of image formation will be discussed elsewhere [18]. A cross section through the image at $y = 0$ plotted in Fig. 2b is closely related to the absorption spectrum of the QWR. At room temperature, this PLE spectrum shows an onset in the range of the QWR emission around 1.459 eV. It has a broad structureless envelope and its maximum at 1.503 eV is blue-shifted with respect to the emission. Calculations of the 1D subband structure [19] indicate that in this 50 nm broad QWR several overlapping transition from valence to conduction subbands contribute to the spectrum [20, 4–6] and give rise to the blue shift of the maximum.

At photon energies higher than 1.515 eV QWR emission is observed for finite lateral distances of the excitation tip from the QWR. In Fig. 2a this gives rise to the bright areas at positive and negative y values. A cross section through this image at

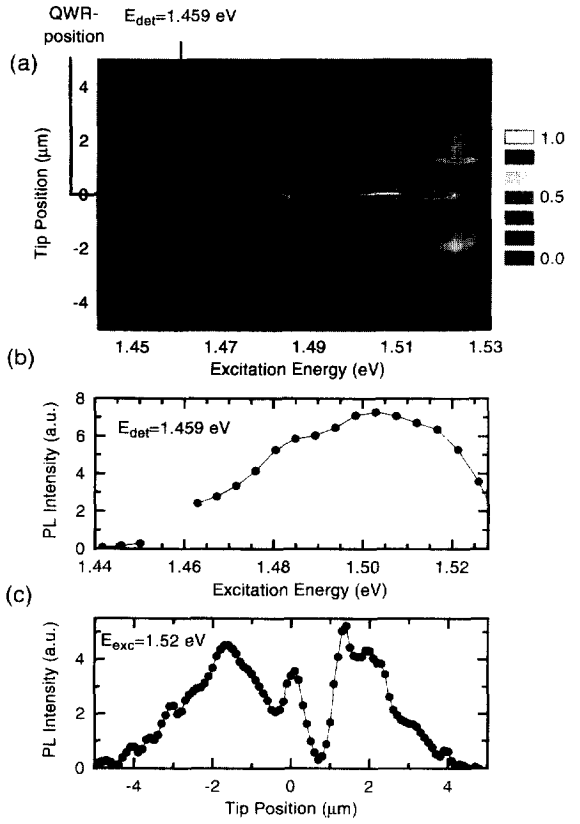

Fig. 2. Near-field PLE spectrum for spatially resolved excitation of the QWR sample through the fiber tip. The intensity of QWR luminescence at 1.459 eV is plotted as a function of excitation energy (abscissa) and of lateral distance between the QWR located at $y = 0$ and the fiber tip (ordinate). For excitation energies below 1.515 eV, electron–hole pairs are excited exclusively in the QWR. At higher photon energies, carriers excited in the quantum-well contribute to the PL signal. (b) Near-field PLE spectrum recorded with excitation at the position of the QWR at ($y = 0$). The arrows indicate the position of interband transitions derived from a theoretical model. (c) Near-field PL line scan for excitation at 1.52 eV.

an excitation energy of 1.52 eV is shown in Fig. 2c. In addition to the maximum at $y = 0$ which is caused by direct excitation of the QWR, two well-separated peaks are resolved in Fig. 2a on the mesa top and bottom. Here, electron–hole pairs are generated by absorption within the flat area GaAs quantum well, undergo diffusive real-space transfer within the QW, and are eventually captured into the QWR where radiative recombination occurs. Because of the diffusion process that precedes carrier capture into the QWR one expects an exponential decrease of the signal with increasing distance from the QWR, on a length scale that is given by the QW diffusion length. A line scan at a fixed excitation energy of 1.52 eV (Fig. 2c) shows such a decrease of the signal for distances $|y| > 2$ μm. Here, the PLE signal decays monotonically and the decay length is about 1.6 mm. The same diffusion length is found with excitation at higher photon energies of 2 eV as discussed below.

At smaller distances, $|y| < 2$ μm, the PLE signal in Fig. 2c *decreases* as the position of the fiber probe approaches the QWR. On the mesa top ($y < 0$), the PLE signal decays gradually, while on the mesa bottom a more pronounced abrupt decrease is found for distances of less than 1.2 μm from the QWR. The signal decreases almost to zero at $y = 0.6$ μm. This spatial variation of the PL intensity is caused by local changes of the quantum-well absorption along the y-direction. In the vicinity of the QWR, the absorption at the band edge of the QW around 1.52 eV is reduced, resulting in a decrease of the signal. The reduction of the QW absorption originates from a local decrease of QW thickness: In the growth process, Ga atoms from this area migrate towards the sidewall and form the (somewhat thicker) quantum wire. Correspondingly, the quantum well is thinned and its absorption is shifted to higher photon energies, giving rise to the observed decrease of the signal in Fig. 2c. The asymmetry of the PLE signal indicates that mesa top and bottom are differently affected by the Ga atom migration. Based on these results, the following qualitative local bandgap map emerges. The wire region with a width of about 50 nm is surrounded by two asymmetric potential barriers, extending to about 1 μm, which separate the QWR and the flat area QW (Fig. 1b) [19].

4. Real-space transfer and carrier trapping

Bearing this information on the local bandstructure in mind, we performed additional near-field photoluminescence (PL) experiments in order to optically analyze microscopic carrier-transport process in this device. At room temperature,

a near-field PL spectrum (Fig. 3) was recorded by locally exciting the sample through the NSOM probe at a fixed photon energy of 1.959 eV. The far-field luminescence was spectrally dispersed and monitored as a function of the tip position with respect to the QWR located at $y = 0$. The tip was again scanned along the lateral y-direction perpendicular to the QWR. In this image, several distinct regions are resolved: (i) QWR luminescence centered at 1.46 eV and around $y = 0$ is resolved at photon energies between 1.45 and 1.50 eV. (ii) PL emission from the embedding GaAs QW centered at 1.522 eV is observed on the flat QW areas of the mesa top and mesa bottom. The QW emission intensity remains approximately constant for tip distances more than 3 μm away from the QWR and decreases for tip positions closer to the sidewall QWR, indicating an efficient carrier capture into the wire. (iii) An additional peak located around $y = 0$ and spectrally centered at 1.526 eV is assigned to electron–hole pair generation near the QWR and an efficient phonon-assisted carrier emission from the QWR into the embedding QW, as is discussed in detail elsewhere [21].

In particular, the spatial dependence of the QWR luminescence peak contains detailed microscopic information on carrier trapping into the QWR. Fig. 4 shows a cross section through Fig. 3 at a fixed detection energy of 1.46 eV. It shows a narrow peak at $y = 0$ that arises from direct excitation of the QWR. In addition, this narrow peak is surrounded by broad wings that extend over lengths of several microns. This occurrence of QWR luminescence after localized QW excitation involves carrier diffusion with the QW and subsequent trapping into the QWR. The logarithmic plot in the insert reveals a monoexponential decrease of the emission intensity at positive and negative tip positions as is expected for diffusive real-space transfer of carriers within the QW. From this plot a diffusion length L_d of 1.6 μm is derived. This diffusion length L_d is determined by the recombination lifetime of the 2D carriers τ_{rec} and the ambipolar diffusion coefficient D as $(L_d)^2 = D\tau_{rec}$. The QW lifetime was measured

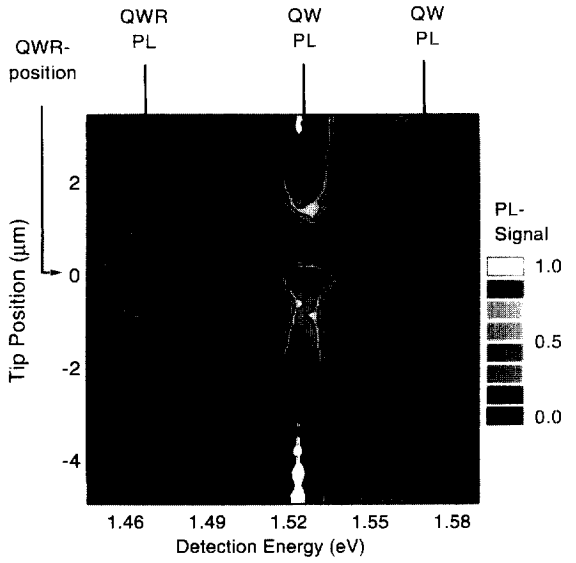

Fig. 3. Spatially resolved room temperature near-field photoluminescence spectrum of the quantum wire heterostructure. The spectrum was recorded for spatially resolved excitation of the sample at 1.959 eV and the tip was scanned along the lateral direction perpendicular to the wire structure. The PL intensity (in a.u.) is plotted as a function of tip position and detection energy. Quantum wire emission is centered around 1.46 eV. Note that, in addition to the flat quantum-well luminescence at 1.522 eV a further, slightly blue shifted, sidewall quantum-well emission is resolved.

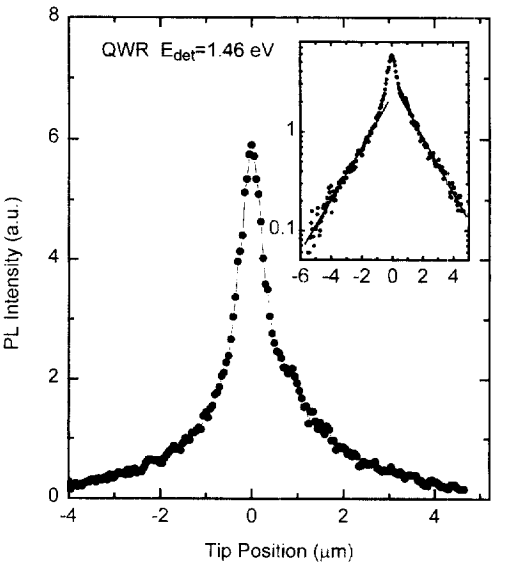

Fig. 4. Spatial profile of QWR photoluminescence (PL). The PL intensity at 1.46 eV is plotted versus the lateral separation of the excitation tip from the QWR (excitation energy 1.959 eV).

to be 2.1 ns by locally exciting the flat area QW far away from the QWR and time resolving the resulting QW luminescence (Fig. 5, upper trace). Thus, the measured luminescence decay was not affected by real-space transfer of carriers. Given the diffusion length L_d of 1.6 μm and using $D = (L_d)^2/t_{rec}$ and the Einstein relation $\mu_{eff} = De/(kT)$ for the effective mobility μ_{eff} of the carriers (e: electron charge, kT thermal energy), one derives values of $D = 12.2\ cm^2/s$ and $\mu_{eff} = 488\ cm^2/(V\ s)$ at $T = 300$ K. This μ_{eff} is very close to the mobility of holes in GaAs at room temperature [22], whereas electron mobilities are significantly higher. We conclude that hole diffusion determines the real-space transfer preceding carrier capture into the QWR.

For local excitation of the QWR (Fig. 5, lower trace), a monoexponential decay of the QWR luminescence intensity was found, giving a recombination lifetime of the QWR of 1.9 ns. This long lifetime is in agreement with theoretically predicted long intrinsic radiative lifetimes of excitons in quantum wires [23] and is another indication for the excellent quality of the MBE grown QWR structure.

A drastically different scenario of carrier transport and trapping is found at low temperatures, as is evident from the spatially resolved PL spectrum recorded at a lattice temperature of 8 K (Fig. 6). As in the room temperature measurement, the sample was locally excited through the NSOM probe at a fixed photon energy of 1.959 eV. Here, the QWR

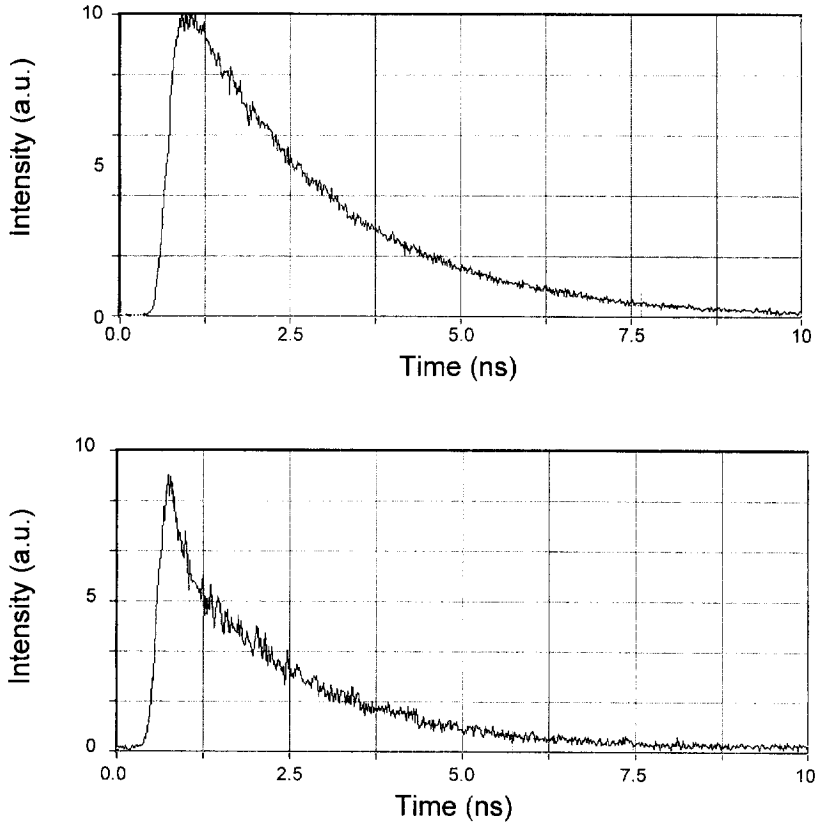

Fig. 5. Time-resolved measurements of the emission from the quantum well (upper trace) and from the quantum wire (lower trace) at room temperature. The luminescence intensity at the maximum of the respective emission spectrum is plotted versus time. The recombination lifetimes are 2.1 ns (QW) and 1.9 ns (QWR).

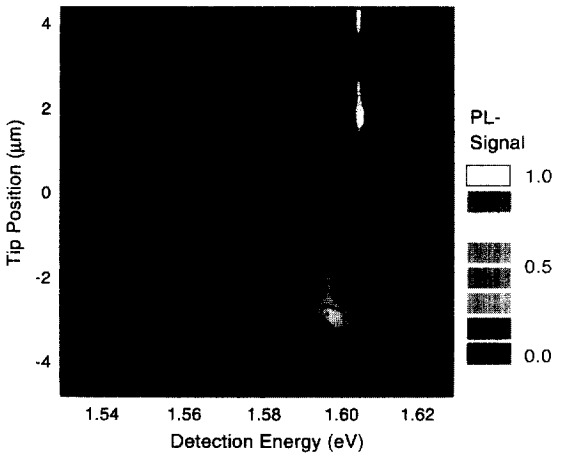

Fig. 6. Spatially resolved near-field photoluminescence (PL) spectrum at 8 K. The spectrum was recorded for spatially resolved excitation of the sample at 1.959 eV and the tip was scanned along the lateral direction perpendicular to the wire structure. The PL intensity (in a.u.) is plotted as a function of tip position and detection energy. Quantum wire emission is centered around 1.545 eV.

emission is centered at 1.545 eV with a spectral width of 4 meV (FWHM). This is in excellent agreement with the recently reported μ-PL spectra for this structure[12]. QW emission is centered around 1.604 eV. The spatial dependence of the QWR luminescence at low-temperatures differs strongly from that at room temperature. QWR emission appears as a single narrow peak centered around $y = 0$ that is well represented by a Gaussian profile with a spatial width of about 800 nm. We note that this width is broader than the spatial resolution of 400 nm in this experiment, as defined by the specific layer structure of our sample and the finite aperture size of the employed NSOM fiber probe of about 300 nm. In contrast to the room temperature measurement, the luminescence intensity at tip distances of more than 1 μm away from the QWR center is less than 5% of the maximum QWR PL. Thus, at low-temperatures carrier capture into the QWR is only observed for localized excitation in the region between the two potential barriers separating the QWR and the flat area QW. Most of the carriers generated there loose their excess energy originating from optical excitation on a picosecond time scale via phonon emission [24], relax into states below the potential barriers and get trapped into the QWR. This is strongly supported by the weak QW emission intensity near $y = 0$. Similarly, carriers that are generated within the flat area quantum-well relax to the lowest QW subbands and undergo diffusive real-space transfer within the quantum well. Unlike at room temperature, thermal activation of carriers across the energetic barriers separating flat area QW and sidewall QWR is suppressed at low temperatures and trapping of carriers generated within the flat area QW is prohibited.

5. Summary and conclusions

In this paper, we demonstrated the potential of near-field spectroscopy for identifying the local energetics of semiconductor nanostructures and analyzing microscopic transport processes in such systems. Near-field spectroscopy advances the achievable spatial resolution in semiconductor spectroscopy towards the 100 nm range and thus allows to spatially select *single* low-dimensional semiconductor nanostructures.

The optical properties and the carrier dynamics of a novel quantum-well embedded quantum wire structure was investigated using variable temperature near-field PL and PLE spectroscopy. The high spatial resolution of the NSOM technique allowed us to separate the absorption spectra of QWR and QW structure and provided direct information on local thickness variations of the embedding QW. The wire region of a width of about 50 nm was shown to be surrounded by two asymmetric potential barriers, extending to about 1 μm, which separate the QWR and the flat area QW. The energetic barriers dominate the carrier trapping mechanism at low temperatures. Here, carrier trapping is efficient only for localized carrier generation near the QWR while thermal activation of carriers across the barriers is prohibited. At room temperature, however, thermal activation across the barriers becomes possible, and carrier trapping is preceded by real-space transfer of carriers in continuum QW states occurring over a length of several micrometers. These experiments underline that variable temperature near-field spectroscopy,

in particular in combination with time-resolved techniques, opens up exciting new possibilities for a microscopic analysis of carrier transport, capture and relaxation processes in low-dimensional semiconductor nanostructures.

References

[1] For a recent overview, the reader is referred to the Proc. 23rd Int. Conf. the Physics of Semiconductors, M. Scheffler, R. Zimmermann (Eds.), World Scientific, Singapore, 1996.
[2] N. Kirstaedter, N.N. Ledentsov, M. Grundmann, D. Bimberg, V.M. Ustinov, S.S. Ruvimov, M.V. Maximov, P.S. Kopév, Zh.I. Alferov, U. Richter, P. Werner, U. Gösele, J. Heidenreich, Electron. Lett. 30 (1996) 1416.
[3] S. Benner, H. Haug, Phys. Rev. B 47 (1993) 15750.
[4] S. Glutsch, D.S. Chemla, Phys. Rev. B 53 (1996) 15902.
[5] S. Glutsch, F. Bechstedt, Phys. Rev. B 47 (1993) 4315.
[6] S. Glutsch, F. Bechstedt, Phys. Rev. B 47 (1993) 6385.
[7] H. Sakaki, Jpn. J. Appl. Phys. 19 (1980) L735.
[8] U. Bockelmann, G. Bastard, Phys. Rev. B 42 (1990) 8947.
[9] J.S. Weiner, H.F. Hess, R.B. Robinson, T.R. Hayes, D.L. Sivco, A.Y. Cho, M. Ranade, Appl. Phys. Lett. 58 (1991) 2402.
[10] R.D. Grober, T.D. Harris, J.K. Trautman, E. Betzig, W. Wegscheider, L. Pfeiffer, K. West, Appl. Phys. Lett. 64 (1994) 1421.
[11] T.D. Harris, D. Gershoni, R.D. Grober, L. Pfeiffer, K.W. West, N. Chand, Appl. Phys. Lett. 68 (1996) 988.
[12] R. Nötzel, M. Ramsteiner, J. Menniger, A. Trampert, H.-P. Schönherr, L. Däweritz, K.H. Ploog, Jpn. J. Appl. Phys. 35 (1996) L297.
[13] R. Nötzel, J. Menniger, M. Ramsteiner, A. Ruiz, H.-P. Schönherr, K.H. Ploog, Appl. Phys. Lett. 68 (1996) 1132.
[14] G. Behme, A. Richter, M. Süptitz, Ch. Lienau, Rev. Sci. Instr. 68 (1997) 3458.
[15] E. Betzig, P.L. Finn, J.S. Weiner, Appl. Phys. Lett. 60 (1992) 2484.
[16] P.C. Yang, Y. Chen, M. Vaez-Irvani, J. Appl. Phys. 71 (1992) 2499.
[17] K. Karrai, R.D. Grober, Appl. Phys. Lett. 66 (1995) 1842.
[18] Ch. Lienau, A. Richter, T. Elsaesser, unpublished.
[19] A. Richter, M. Süptitz, Ch. Lienau, T. Elsaesser, Surf. Interface Anal., 1997, in press.
[20] A.N. Forshaw, D.M. Whittaker, Phys. Rev. B 54 (1996) 8794.
[21] A. Richter, M. Süptitz, Ch. Lienau, T. Elsaesser, M. Ramsteiner, R. Nötzel, K.H. Ploog, Phys. Rev. Lett. 79 (1997) 2145
[22] D.C. Look et al., Properties of GaAs, INSPEC, London, 1990, p.97.
[23] D.S. Citrin, Phys. Rev. Lett. 69 (1992) 3393.
[24] J. Shah, Ultrafast Spectroscopy of Semiconductors and Semiconductor Nanostructures, Springer, Berlin, 1996.